

Decomposition Functions for Interconnected Mixed Monotone Systems

Matthew Abate, *Student Member, IEEE* and Samuel Coogan, *Member, IEEE*

Abstract—A dynamical system is mixed monotone when there exists a related decomposition function that separates the system dynamics into cooperative and competitive state interactions. Such a decomposition enables, *e.g.*, efficient computation of robust reachable sets and forward invariant sets, but obtaining a decomposition function can be challenging. In this letter, we present a method for obtaining a decomposition function for a system that can be represented as an interconnection of subsystems with known decomposition functions. We further extend this approach using tools from interval reachability analysis to accommodate systems with outputs and we provide also conditions for when the system’s unique tight decomposition function is obtained via this approach. We demonstrate this methodology for computing decomposition functions with an example of a 3-dimensional unicycle model and with a case study of a 7-dimensional nonlinear spacecraft system defined as an interconnection of subsystems and feedback controllers. Reachable sets for the systems are then computed using their decomposition functions and the standard tools from mixed monotone systems theory.

Index Terms—Networked Control Systems, Uncertain Systems, Nonlinear Output Feedback

I. INTRODUCTION

A dynamical system, possibly subject to a nondeterministic disturbance input, is mixed monotone when there exists a related decomposition function that separates the system dynamics into cooperative and competitive state interactions. Mixed monotonicity applies to continuous-time systems [1]–[4], discrete-time systems [5], as well as systems with disturbances [6]–[8], and it generalizes the *monotonicity* property of dynamical systems for which trajectories maintain a partial order over states [9], [10].

For an n -dimensional mixed monotone system with a disturbance input, it is possible to construct a $2n$ -dimensional monotone embedding system from the decomposition function. This embedding system contains no disturbances and trajectories of the embedding system provide bounds for reachable sets of the initial system [7], [8], a result that has been applied for, *e.g.*, efficient controller verification and synthesis [11], [12], as well as in online safety applications [13], [14]. The monotonicity of the embedding system can also be exploited for the computation of forward invariant sets and attractive sets for the initial system [8], [15].

This work was partially supported by the Air Force Office of Scientific Research under grant FA9550-19-1-0015 and by the NSF under grants #1749357 and #1836932.

M. Abate is with the School of Mechanical Engineering and the School of Electrical and Computer Engineering, Georgia Institute of Technology, Atlanta, 30332, USA Matt.Abate@GaTech.edu.

S. Coogan is with the School of Electrical and Computer Engineering and the School of Civil and Environmental Engineering, Georgia Institute of Technology, Atlanta, 30332, USA Sam.Coogan@GaTech.edu.

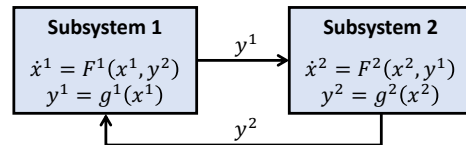


Fig. 1: We present a method for computing decomposition functions for mixed monotone systems that are the interconnection of subsystems, as shown above for the case with two subsystems and no disturbance inputs.

A challenge in using mixed monotone system theory in applications is in identifying a suitable decomposition function for the system. Certain algorithms exist for computing decomposition functions from, *e.g.*, bounds on the system Jacobian matrix [3], [7] or domain specific knowledge [4], [15], and it is known that all systems with Lipschitz continuous vector field are mixed monotone with respect to a unique tight decomposition function that provides tighter approximations of reachable sets than any other decomposition function for the same system when used with the standard mixed monotone system tools [16]. However, analogous to searching for Lyapunov functions, finding a closed-form decomposition function for complex systems can be difficult.

The main result of this letter is a method for obtaining a decomposition function for a system that can be represented as the interconnection of subsystems with known decomposition functions as in Figure 1. This approach can significantly reduce the complexity of computing tight decomposition functions in closed form, and we show how tools from interval reachability analysis [17], [18] can be included in the method to allow for computing reachable sets for systems with outputs or systems subject to state feedback controllers. Conceptually, our approach is similar to, *e.g.*, methods that compute composite Lyapunov functions from a collection of subsystem storage functions using dissipativity theory [19]. A benefit of this modular approach to obtaining decomposition functions is that changing a subsystem or its decomposition function leads immediately to a new composite decomposition function for the interconnection, and we demonstrate by an example how a state transformation of one subsystem improves reachable set approximations of the composite system.

We demonstrate the results of this letter with an example of a 3-dimensional unicycle model and through a case study of a 7-dimensional nonlinear spacecraft system defined as an interconnection of subsystems and feedback controllers. In the case study we compute two approximations of the reachable set of a nonlinear output function using the resulting composite decomposition function obtained from two choices of subsystem decomposition functions for the spacecraft.

II. NOTATION

Let (x, y) denote the vector concatenation of $x, y \in \mathbb{R}^n$, i.e., $(x, y) := [x^T y^T]^T \in \mathbb{R}^{2n}$, and let \preceq denote the componentwise vector order, i.e., $x \preceq y$ if and only if $x_i \leq y_i$ for all $i \in \{1, \dots, n\}$ where vector components are indexed via subscript. Given $x, y \in \mathbb{R}^n$ with $x \preceq y$,

$$[x, y] := \{z \in \mathbb{R}^n \mid x \preceq z \text{ and } z \preceq y\} \quad (1)$$

denotes the hyperrectangle defined by the endpoints x and y . We also allow $x \in \mathbb{R}^n \cup \{-\infty\}$ and $y \in \mathbb{R}^n \cup \{\infty\}$, in which case $[x, y]$ defines an *extended hyperrectangle*, that is, a hyperrectangle with possibly infinite extent in some coordinates. Given $a = (x, y) \in \mathbb{R}^{2n}$ with $x \preceq y$, let $\llbracket a \rrbracket$ denote the hyperrectangle formed by the first and last n components of a , $\llbracket a \rrbracket := [x, y]$.

III. PRELIMINARIES

Consider a dynamical system given by

$$\dot{x} = F(x, w) \quad (2)$$

for Lipschitz F where $x \in \mathcal{X} \subseteq \mathbb{R}^n$ and $w \in \mathcal{W} \subset \mathbb{R}^m$ denote the system state and a bounded time-varying auxiliary input, respectively. We assume \mathcal{X} is an extended hyperrectangle with nonempty interior and $\mathcal{W} := [\underline{w}, \bar{w}]$ is a hyperrectangle for some $\underline{w}, \bar{w} \in \mathbb{R}^m$ with $\underline{w} \preceq \bar{w}$.

For $t \geq 0$, let $\Phi^F(t; x, \mathbf{w})$ denote the state of (2) reached at time t starting from $x \in \mathcal{X}$ at time 0 under the piecewise continuous input $\mathbf{w} : [0, t] \rightarrow \mathcal{W}$. Throughout, we always assume that time-varying input signals such as \mathbf{w} are piecewise continuous so that, in particular, $\Phi^F(t; x, \mathbf{w})$ is unique when it exists. We do not a priori require $\Phi^F(t; x, \mathbf{w})$ to exist for all t ; however, existence of $\Phi^F(t; x, \mathbf{w})$ implicitly means that $\Phi^F(\tau; x, \mathbf{w}) \in \mathcal{X}$ for all $0 \leq \tau \leq t$. Denote also by

$$R^F(t; A) := \left\{ \Phi^F(t; x, \mathbf{w}) \in \mathcal{X} \mid x \in A \text{ for some } \mathbf{w} : [0, t] \rightarrow \mathcal{W} \right\} \quad (3)$$

the *time- t reachable set* of (2), which is the set of states that are reachable by (2) in time $t \geq 0$ from $A \subseteq \mathcal{X}$ under some input.

Definition 1. [20] Given a locally Lipschitz continuous function $d : \mathcal{X} \times \mathcal{W} \times \mathcal{X} \times \mathcal{W} \rightarrow \mathbb{R}^n$, the system (2) is *mixed monotone with respect to d* if for all $x, \hat{x} \in \mathcal{X}$ and all $w, \hat{w} \in \mathcal{W}$ the following hold:

- $d(x, w, x, w) = F(x, w)$,
- $\frac{\partial d_i}{\partial x_j}(x, w, \hat{x}, \hat{w}) \geq 0$ for all $i, j \in \{1, \dots, n\}$ with $i \neq j$,
- $\frac{\partial d_i}{\partial \hat{x}_j}(x, w, \hat{x}, \hat{w}) \leq 0$ for all $i, j \in \{1, \dots, n\}$,
- $\frac{\partial d_i}{\partial w_k}(x, w, \hat{x}, \hat{w}) \geq 0$ and $\frac{\partial d_i}{\partial \hat{w}_k}(x, w, \hat{x}, \hat{w}) \leq 0$ for all $i \in \{1, \dots, n\}$ and all $k \in \{1, \dots, m\}$. ■

If (2) is mixed monotone with respect to d , d is said to be a *decomposition function* for (2), and when d is clear from context we simply say (2) is mixed monotone. In the special case when the system (2) is mixed monotone with respect to d given by $d(x, w, \hat{x}, \hat{w}) = F(x, w)$, Definition 1 recovers

familiar conditions establishing *monotonicity*, as defined in [9]. A common interpretation of monotonicity is requiring cooperative interaction among all state variables, and mixed monotonicity provides an extension allowing for competitive effects captured by the hatted variables. Last, when F in (2) depends only on the input w so that $\dot{x} = F(w)$ we omit the first and third inputs in d so that now (2) is mixed monotone with respect to $d(w, \hat{w})$.

An important feature of mixed monotone systems that we exploit in this work is that hyperrectangular over-approximations of reachable sets can be efficiently computed by considering a deterministic auxiliary embedding system constructed from the decomposition function. Given d ,

$$\begin{bmatrix} \dot{x} \\ \dot{\hat{x}} \end{bmatrix} = E(x, \hat{x}) = \begin{bmatrix} d(x, \underline{w}, \hat{x}, \bar{w}) \\ d(\hat{x}, \bar{w}, x, \underline{w}) \end{bmatrix} \quad (4)$$

is the *embedding system relative to d* and E is the *embedding function*. We denote by $\Phi^E(t; a)$ the state of (4) reached at time t when beginning at state $a \in \mathcal{X} \times \mathcal{X}$ at time 0. Unlike the initial system (2), which is nondeterministic due to the effect of the unknown input, the embedding system (4) contains no input and trajectories of (4) provide bounds on the reachable set of (2), as discussed next in Proposition 1.

Proposition 1. [20] *Let (2) be mixed monotone with respect to d and consider $\llbracket a \rrbracket \subset \mathcal{X}$. If $\Phi^E(\tau; a) \in \mathcal{X} \times \mathcal{X}$ for all $0 \leq \tau \leq t$, then $R^F(t; \llbracket a \rrbracket) \subseteq \llbracket \Phi^E(t; a) \rrbracket$.*

Proposition 1 provides an efficient algorithm for over-approximating reachable sets for (2): a simulation of the embedding system for time horizon t , starting from state (x, \bar{x}) , identifies a hyperrectangular over-approximation of $R^F(t; [x, \bar{x}])$ where the largest and smallest points in the rectangular approximation are taken to be the first n and last n coordinates of the simulation endpoint $\Phi^E(t; (x, \bar{x}))$.

IV. MIXED MONOTONICITY AND REACHABILITY ANALYSIS FOR SYSTEMS WITH OUTPUTS

We have discussed already in Section III how a decomposition function for (2) enables the efficient over-approximation of $R^F(t; A)$ with rectangles. We study next a similar problem, concerning reachability analysis for systems with outputs. In particular, we consider

$$\begin{aligned} \dot{x} &= F(x, w) \\ y &= g(x) \end{aligned} \quad (5)$$

where now $y \in \mathbb{R}^p$ denotes the system output, and we are interested in computing an over-approximation of

$$R^g(t; A) := \left\{ g(\Phi^F(t; x, \mathbf{w})) \in \mathbb{R}^p \mid x \in A \text{ for some } \mathbf{w} : [0, t] \rightarrow \mathcal{W} \right\}. \quad (6)$$

Existing results for approximating reachable sets using mixed monotone systems theory apply only to systems without outputs as in (2) and are not applicable to (5). In this section, to accommodate system outputs in the procedure, we leverage tools from interval analysis [17], [18]. Denote by

$$\begin{aligned} \mathbb{IX} &:= \{[x, \bar{x}] \subseteq \mathcal{X} \mid x, \bar{x} \in \mathcal{X}, x \preceq \bar{x}\} \subset 2^{\mathcal{X}} \\ \mathbb{IIR}^p &:= \{[y, \bar{y}] \subseteq \mathbb{R}^p \mid y, \bar{y} \in \mathbb{R}^p, y \preceq \bar{y}\} \subset 2^{\mathbb{R}^p} \end{aligned} \quad (7)$$

the sets of interval subsets of \mathcal{X} and \mathbb{R}^p respectively. The following definition is from [18, Sec. 2.4.1].

Definition 2 (inclusion function). Given $g : \mathcal{X} \rightarrow \mathbb{R}^p$, the interval function $G : \mathbb{I}\mathcal{X} \rightarrow \mathbb{I}\mathbb{R}^p$ is an *inclusion function* for g if for all hyperrectangles $A \in \mathbb{I}\mathcal{X}$

$$G(A) \supseteq \{g(x) \in \mathbb{R}^p \mid x \in A\}. \quad (8)$$

There are known similarities between mixed monotone systems theory and interval analysis, as highlighted recently in [21]. Both theories provide efficient techniques for over-approximating reachable sets using hyperrectangles and, of particular importance, inclusion functions can be generated from decomposition functions. That is, given a dynamical system

$$\dot{y} = g(x), \quad (9)$$

where $y \in \mathbb{R}^p$ is the state and $x \in \mathcal{X}$ is the input, the interval function

$$G([\underline{x}, \bar{x}]) := [d(\underline{x}, \bar{x}), d(\bar{x}, \underline{x})] \quad (10)$$

is an inclusion function for g when $d(x, \hat{x})$ is a decomposition function for (9). Moreover, Proposition 1 combined with Definition 2 leads to the following corollary.

Corollary 1. *Let (2) be mixed monotone with respect to d and let G be an inclusion function for g . Choose $A := [\underline{x}, \bar{x}] \subset \mathcal{X}$. If $\Phi^E(t; (\underline{x}, \bar{x})) \in \mathcal{X} \times \mathcal{X}$ for all $\tau \in [0, t]$ then*

$$R^E(t; A) \subseteq G([\Phi^E(t; (\underline{x}, \bar{x}))]), \quad (11)$$

where $\Phi^E(t; a)$ is the state transition function of the embedding system (4) formed from d .

It is important here to discuss the *tightness* of reachable set approximations in the context of Corollary 1. Mixed monotone reachability methods exhibit a useful *nesting* property allowing one to reason about the tightness of decomposition functions; that is, when d is a decomposition function for (2), and when $A = [\underline{x}, \bar{x}]$ and $B = [\underline{y}, \bar{y}]$ are hyperrectangles with $A \subseteq B$, it holds that

$$[\Phi^E(t; (\underline{x}, \bar{x}))] \subseteq [\Phi^E(t; (\underline{y}, \bar{y}))], \quad (12)$$

for all $t \geq 0$. Equivalently, when $A \subseteq B$, the hyperrectangular approximation containing $R^E(t; A)$ will contain that of $R^E(t; B)$ for all $t \geq 0$. This property is explored in [16] where it is shown that all system (2) are mixed monotone with respect to a unique *tight* decomposition function that provides tighter approximations of reachable sets when used with Proposition 1 than any other decomposition function for the same system. The nesting property detailed above, however, is not necessarily exhibited by inclusion functions; indeed, the hypothesis of Definition 2 allows for inclusion functions G so that

$$G(A) \not\subseteq G(B) \quad (13)$$

when $A \subseteq B$. Thus, even when a tight decomposition function d is used with Corollary 1 there may exist another decomposition function d' for the same system so that

$$G([\Phi^E(t; (\underline{x}, \bar{x}))]) \not\subseteq G([\Phi^{E'}(t; (\underline{x}, \bar{x}))]), \quad (14)$$

i.e., the tight decomposition function d loses tightness guarantees when used with Corollary 1.

Nonetheless, we argue that any useful inclusion function should exhibit the nesting property detailed above, and in the examples and discussion provided later, we assume always that inclusion functions G are chosen so that $A \subseteq B$ implies $G(A) \subseteq G(B)$. This is the case, in particular when G is constructed from a decomposition function for $\dot{y} = g(x)$ using (10). In the following section, we sometimes represent inclusion functions $G : \mathbb{I}\mathcal{X} \rightarrow \mathbb{I}\mathcal{X}$ using the function $G : \{(x, \hat{x}) \in \mathcal{X} \times \mathcal{X} \mid x \preceq \hat{x} \text{ or } \hat{x} \preceq x\} \rightarrow \mathcal{X}$ defined by

$$G([\underline{x}, \bar{x}]) := [G(\underline{x}, \bar{x}), G(\bar{x}, \underline{x})] \quad (15)$$

and, in this case, we assume always $G(x, x) = g(x)$.

V. MIXED MONOTONICITY FOR INTERCONNECTED SYSTEMS

The main result of this letter is to present a method for obtaining a decomposition function for interconnected systems using decomposition functions for the subsystems. We consider N systems, interconnected via nonlinear feedback

$$\begin{aligned} \text{Subsystem 1: } \dot{x}^1 &= F^1(x^1, y, w) \\ \text{Subsystem 2: } \dot{x}^2 &= F^2(x^2, y, w) \\ &\vdots \\ \text{Subsystem } N: \dot{x}^N &= F^N(x^N, y, w) \\ \text{Feedback: } y &= g(x^1, \dots, x^N) \end{aligned} \quad (16)$$

where $\mathcal{X}^i \subseteq \mathbb{R}^{n_i}$ for $i \in \{1, \dots, N\}$ denotes the state space of the i^{th} subsystem, $y \in \mathbb{R}^p$ is a feedback term, and the input space of the interconnection is $\mathcal{W} \subset \mathbb{R}^m$. For the case of two subsystems, this problem setting is depicted in Figure 1. The full interconnected dynamics are denoted

$$\dot{x} = F(x, w) := \begin{bmatrix} F^1(x^1, g(x), w) \\ \vdots \\ F^N(x^N, g(x), w) \end{bmatrix} \quad (17)$$

with state $x := (x^1, \dots, x^N) \in \mathcal{X} := \mathcal{X}^1 \times \dots \times \mathcal{X}^N \subseteq \mathbb{R}^n$ and where $n := \sum_{i=1}^N n_i$.

We show next how a decomposition function for the interconnected system (17) is constructed from decomposition functions for the individual subsystems, thus allowing, *e.g.*, the efficient over-approximation of reachable sets for (17). In Theorem 1 and in the following discussion, we use the notation $a_{[i:b]}$ to denote a vector a whose i^{th} element has been replaced by the i^{th} element of the vector b .

Theorem 1. *Consider (17) and assume that for all $i \in \{1, \dots, N\}$ the i^{th} subsystem*

$$\dot{x}^i = F^i(x^i, y, w) \quad (18)$$

is mixed monotone with respect to

$$d^i(x^i, y, w, \hat{x}^i, \hat{y}, \hat{w}) \quad (19)$$

where $y \in \mathcal{Y} \subseteq \mathbb{R}^p$ is viewed as a system input. Let G be an inclusion function for g . Then the system (17) is mixed monotone with respect to d defined elementwise by

$$d_j(x, w, \hat{x}, \hat{w}) := d_k^i(x^i, G(x, \hat{x}_{[j:x]}), w, \hat{x}^i, G(\hat{x}_{[j:x]}, x), \hat{w}). \quad (20)$$

for $j \in \{1, \dots, n\}$ and where x_j is the k^{th} element of x^i , i.e., the k^{th} state of the i^{th} subsystem.

Proof: We show that d is a decomposition function for (17) by showing that d satisfies the four conditions in Definition 1. Since d^i is a decomposition function for the i^{th} subsystem, and since $G(x, x) = g(x)$, it holds that $d(x, w, x, w) = F(x, w)$ for all $x \in \mathcal{X}$ and $w \in \mathcal{W}$. Therefore d from (24) satisfies the first condition in Definition 1. To show that d from (24) satisfies conditions 2–4 of Definition 1, observe that $G(x, \hat{x})$ is increasing in its first argument and decreasing in its second argument, so that, e.g., $\frac{\partial d_i}{\partial x_j}(x, w, \hat{x}, \hat{w}) \geq 0$ for all $i \neq j$ and the remaining derivative conditions are satisfied similarly. ■

It is instructive to consider the specialization of Theorem 1 to the case of one subsystem, which may represent, e.g., a closed-loop controlled dynamical system.

Corollary 2. Consider a controlled dynamical system under feedback

$$\dot{x} = F(x, u(x), w) \quad (21)$$

where now the second input in (21) is understood to represent a control input, and $u : \mathcal{X} \rightarrow \mathbb{R}^m$ is an explicitly defined feedback control policy. If the system $\dot{x} = F(x, y, w)$ is mixed monotone with respect to $d'(x, y, w, \hat{x}, \hat{y}, \hat{w})$, and $U(x, \hat{x})$ is an inclusion function for $u(x)$, then the system (21) is mixed monotone with respect to d defined element wise by

$$d_j(x, w, \hat{x}, \hat{w}) := d'_j(x, U(x, \hat{x}_{[j:x]}), w, \hat{x}, U(\hat{x}_{[j:x]}, x), \hat{w}). \quad (22)$$

In practice, in the experience of the authors, Theorem 1 and Corollary 2 provide the dominant and most tractable method for obtaining decomposition functions for nonlinear systems with more than a few state dimensions. Moreover, in some cases, this method leads to tight decompositions functions, as formalized next in Theorem 2.

Theorem 2. Consider a system interconnection as in (17). Assume that for each $i \in \{1, \dots, N\}$, the i^{th} subsystem can be written as

$$\dot{x}^i = F^i(x^i, g(x), w) = F^i(x^i, g^i(x), w) \quad (23)$$

where $g^i(x)$ does not depend on x^i and for all j , if $g_k^i(x)$ depends on x_j for some k , then $g_\ell^i(x)$ does not depend on x_j for all $\ell \neq k$. Let $d^i(x, y, w, \hat{x}, \hat{y}, \hat{w})$ be the tight decomposition function for $\dot{x}^i = F^i(x^i, y^i, w)$ and let $d^{g^i}(w, \hat{w})$ be a tight decomposition function for $\dot{y} = g^i(w)$. Then the tight decomposition function for (17) is defined elementwise by

$$d_j(x, w, \hat{x}, \hat{w}) := d_k^i(x^i, d^{g^i}(x, \hat{x}), w, \hat{x}^i, d^{g^i}(\hat{x}, x), \hat{w}) \quad (24)$$

for $j \in \{1, \dots, n\}$ and where x_j is the k^{th} element of x^i , i.e., the k^{th} state of the i^{th} subsystem.

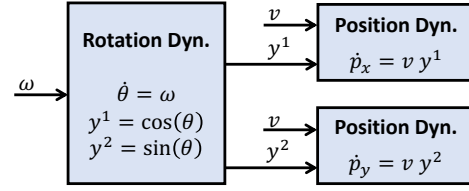


Fig. 2: Example 1: Depiction of the kinematic unicycle model (26) as an interconnection.

The proof of Theorem 2 involves showing that for all j

$$d_j(x, w, \hat{x}, \hat{w}) = \begin{cases} \min_{\substack{\psi \in [\hat{x}, \hat{x}] \\ \psi_j = x_j \\ y \in [d^h(x, \hat{x}), d^h(\hat{x}, x)] \\ z \in [w, \hat{w}]} F_k^i(\psi^i, y, z) & \text{if } (x, w) \preceq (\hat{x}, \hat{w}), \\ \max_{\substack{\psi \in [\hat{x}, \hat{x}] \\ \psi_j = x_j \\ y \in [d^h(\hat{x}, x), d^h(x, \hat{x})] \\ z \in [\hat{w}, w]} F_k^i(\psi^i, y, z) & \text{if } (\hat{x}, \hat{w}) \preceq (x, w). \end{cases} \quad (25)$$

See [16, Equation (16)]. We demonstrate the application of Theorem 2 in the following example where we compute a tight decomposition function for the kinematic unicycle model¹.

Example 1. Consider the kinematic unicycle model

$$\begin{aligned} \dot{p}_x &= v \cos \theta \\ \dot{p}_y &= v \sin \theta \\ \dot{\theta} &= \omega \end{aligned} \quad (26)$$

with state $x = (p_x, p_y, \theta) \in \mathcal{X} = \mathbb{R}^3$ and input $u = (v, \omega) \in \mathcal{W}$. To construct a tight decomposition function for (26), we represent the model as a system interconnection as depicted graphically in Figure 2. Note that, e.g., $\dot{p}_x = F^1(p_x, g^1(\theta), w)$ where $g^1(\theta) = \cos(\theta)$, so that the interconnection satisfies the hypothesis of Theorem 2. Tight decomposition functions for the three scalar subsystems are formed and we construct inclusion functions for $\cos(\theta)$ and $\sin(\theta)$ using tight decomposition functions for the systems

$$\dot{y}^1 = \cos(w) \text{ and } \dot{y}^2 = \sin(w), \quad (27)$$

respectively. A tight decomposition function for (26) is now obtained by applying Theorem 2, and Proposition 1 implies that the reachable set of (26) is efficiently overapproximated via a single simulation of the embedding system (4). An example is shown in Figure 3 where we compute $R^F(t; A)$ for $t = 6$, $A = [-1, 1]^2 \times [\frac{\pi}{3}, \frac{\pi}{2}]$ and $\mathcal{W} = [0.9, 1] \times [-0.1, 0.1]$. ■

VI. CASE STUDY

We now demonstrate the application of Theorem 1 and Corollary 2 on a 7-dimensional spacecraft system. Reachable

¹The code that accompanies Example 1 and generates the figures in this work is publicly available through the GaTech FactsLab GitHub: https://github.com/gtfactslab/Abate_LCSS2021. An explicit representation of the tight decomposition function for (26) is also provided.

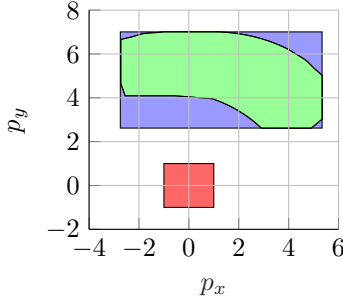


Fig. 3: Example 1: computing reachable sets for (26) by applying Theorem 1. A hyperrectangular over-approximations of $R^F(6; A)$ is computed, with initial set $A = [-1, 1]^2 \times [\frac{\pi}{3}, \frac{\pi}{2}]$ and where $\mathcal{W} = [0.9, 1] \times [-0.1, 0.1]$. The over-approximation of $R^F(6; A)$ attained from applying Theorem 1 is shown in blue, projected onto the p_x - p_y plane. The initial set A is shown in red, and the true system reachable set $R^F(6; A)$, which was computed via exhaustive simulation, is shown in green.

sets for the spacecraft are then computed in an output space by applying Corollary 1.

Consider a torque-controlled spacecraft in unconstrained rotational motion. The spacecraft is modeled with state $x = (q, \omega) \in \mathbb{R}^7$ and control input $u \in \mathbb{R}^3$, where the orientation of the spacecraft is captured by the quaternion vector $q \in \mathbb{H} \subset \mathbb{R}^4$ and the angular velocity is captured by $\omega \in \mathbb{R}^3$. The quaternion vector $q = (q_0, q_1, q_2, q_3)$ defines the orientation of a body-fixed reference frame \mathcal{F}_B with respect to an inertial frame \mathcal{F}_I , as depicted in Figure 4, and the components of $\omega = (\omega_x, \omega_y, \omega_z)$ and $u = (u_1, u_2, u_3)$ are expressed in the body frame \mathcal{F}_B . Denote also by $J \in \mathbb{R}^{3 \times 3}$ the inertia matrix of the spacecraft, taken with respect to \mathcal{F}_B .

Fixed to the spacecraft is a boresight sensor, whose orientation is described by

$$\theta(x) = \arccos(1 - 2q_1^2 - 2q_2^2). \quad (28)$$

The goal of this study is to over-approximate $R^\theta(t; A)$ —the reachable set of spacecraft in the space of line-of-sight angles—by applying Theorem 1 and Corollary 1.

The dynamics of the spacecraft can be described as the interconnection between two subsystems, as depicted graphically in Figure 5 and described below.

Subsystem 1: The angular velocity dynamics are given by

$$\dot{\omega} = J^{-1}(-\omega \times J\omega + u + w) \quad (29)$$

where $u \in \mathbb{R}^3$ is the control input and where $w \in \mathcal{W} \subset \mathbb{R}^3$ denotes a bounded nondeterministic disturbance input. We construct a decomposition function for the velocity dynamics (29) by applying the results of [15], which provides an algorithm for constructing decomposition functions for systems defined by polynomial vector fields.

Subsystem 2: The quaternion dynamics are given by

$$\dot{q} = Q(q)\omega \quad (30)$$

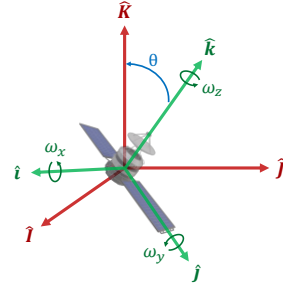


Fig. 4: Case Study: Depiction of the spacecraft system. The body-fixed reference frame \mathcal{F}_B is shown in green and inertial reference frame \mathcal{F}_I is shown in red. The line-of-sight angle θ from (28) is shown in blue.

where $Q(q)$ is the quaternion kinematic matrix, given by

$$Q(q) := \frac{1}{2} \begin{bmatrix} -q_1 & -q_2 & -q_3 \\ q_0 & -q_3 & q_2 \\ q_3 & q_0 & -q_1 \\ -q_2 & q_1 & q_0 \end{bmatrix}. \quad (31)$$

When ω is viewed as an input, the quaternion dynamics (30) are mixed monotone with respect to a tight decomposition attained in closed form.

Feedback Controller: We consider the feedback controller

$$u^{\text{ideal}}(x) = \omega \times J\omega - k_p J\eta - k_d J\omega \quad (32)$$

for suitable controller gains $k_p > 0$, $k_d > 0$ and

$$\eta := \begin{bmatrix} 2(q_2 q_3 + q_0 q_1) \\ 2(q_0 q_2 - q_1 q_3) \\ 0 \end{bmatrix}. \quad (33)$$

An inclusion function for $u^{\text{ideal}}(x)$ is formed using a decomposition function for the mixed monotone system $\dot{y} = u^{\text{ideal}}(x)$, as described in Section IV.

Saturation Function: Before being applied to the second subsystem, the feedback control input (32) is passed through a saturation function

$$u^{\text{applied}} = \sigma(u^{\text{ideal}}) := \frac{1}{2} \tanh(2u^{\text{ideal}}), \quad (34)$$

where the hyperbolic tangent function \tanh in (34) is understood to apply componentwise. The system $\dot{y} = \sigma(w)$ is a monotone system, and therefore an inclusion function for $\sigma(w)$ is given by $\Sigma([w, \bar{w}]) = [\sigma(\underline{w}), \sigma(\bar{w})]$.

Thus, Theorem 1 can now be applied to form a decomposition function for the feedback-interconnected system, from the decomposition functions for (29)–(30) and the inclusion functions for (32) and (34). An example is shown in Figure 6 where we apply Corollary 1 with an inclusion function for (28) to compute an over-approximation of $R^\theta(t; x_0)$ on the time interval $t \in [0, 15]$, where $x_0 = (q_0, \omega_0)$ with

$$q_0 = (\sqrt{3}/2, 0.5, 0, 0) \text{ and } \omega_0 = (0.1, 0.1, 0.1), \quad (35)$$

the disturbance bound is $\mathcal{W} = [-5 \times 10^{-3}, 5 \times 10^{-3}]^3$, the controller gains are $k_p = 0.6$ and $k_d = 2.25$, and the inertia matrix is given by $J = \begin{bmatrix} 17.5 & -0.8 & 0.3 \\ -0.8 & 14.9 & 0.4 \\ 0.3 & 0.4 & 20.8 \end{bmatrix}$.

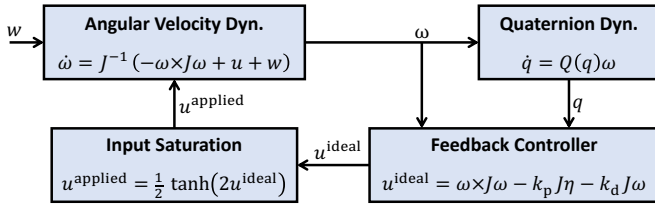


Fig. 5: Case Study: Depiction of the spacecraft model as an interconnection amongst subsystems.

A benefit of considering systems (2) as a feedback interconnection comes from the modular nature of the system representation, so that changing a subsystem or its decomposition function leads immediately to a new composite decomposition function for the interconnection. In particular, state transformations of the subsystem’s dynamical models allow for improved fidelity in the approximation of reachable sets: an observation made in [22] for the case with no interconnections. To demonstrate this assertion, we next consider a linear transformation on the statespace of the first subsystem $\omega' = J\omega$ so that the dynamics of the first subsystem become

$$\dot{\omega}' = -J^{-1}\omega' \times \omega' + u + w \quad (36)$$

where $u \in \mathbb{R}^3$ and $w \in \mathcal{W}$ retain their definitions from (29), and the angular velocity $\omega = J^{-1}\omega' \in \mathbb{R}^3$ is now a system output. We show in Figure 6 how this approach reduces conservatism in the approximation of reachable sets, where we recompute $R^\theta(t; x_0)$ for the parameters taken previously.

VII. CONCLUSION

In this work, we show how decomposition functions are formed for systems defined as an interconnection of subsystems, by computing decomposition functions for the subsystems individually. This simplifies the procedure for identifying decomposition functions for complex systems, and we show also how tools from interval reachability analysis can be included in the approach to allow for, e.g., computing reachable sets for systems with outputs.

REFERENCES

- [1] D. Angeli, G. A. Enciso, and E. D. Sontag, “A small-gain result for orthant-monotone systems under mixed feedback,” *Systems & Control Letters*, vol. 68, pp. 9–19, 2014.
- [2] G. Enciso, H. Smith, and E. Sontag, “Nonmonotone systems decomposable into monotone systems with negative feedback,” *Journal of Differential Equations*, vol. 224, no. 1, pp. 205–227, 2006.
- [3] L. Yang, O. Mickelin, and N. Ozay, “On sufficient conditions for mixed monotonicity,” *IEEE Transactions on Automatic Control*, vol. 64, pp. 5080–5085, Dec 2019.
- [4] S. Coogan and M. Arcak, “Stability of traffic flow networks with a polytree topology,” *Automatica*, vol. 66, pp. 246–253, Apr. 2016.
- [5] H. L. Smith, “The discrete dynamics of monotonically decomposable maps,” *Journal of Mathematical Biology*, vol. 53, p. 747, May 2006.
- [6] P. Meyer and D. V. Dimarogonas, “Hierarchical decomposition of LTL synthesis problem for nonlinear control systems,” *IEEE Transactions on Automatic Control*, vol. 64, pp. 4676–4683, Nov 2019.
- [7] P.-J. Meyer, A. Devonport, and M. Arcak, “Tira: Toolbox for interval reachability analysis,” in *Proceedings of the 22nd ACM International Conference on Hybrid Systems: Computation and Control, HSCC '19*, p. 224–229, Association for Computing Machinery, 2019.

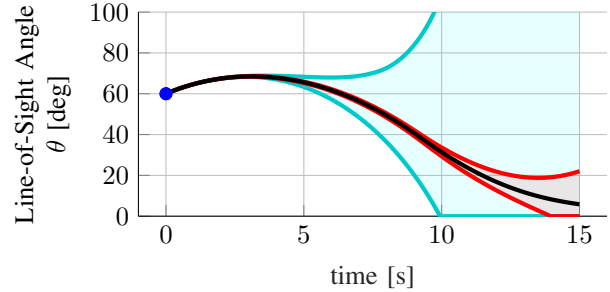


Fig. 6: Case Study: Computing reachable sets for (29)–(30) by applying Theorem 1 and Corollary 1. Two hyperrectangular over-approximations of $R^\theta(t; x_0)$ are computed, with initial state $x_0 = (q_0, \omega_0)$ given by (35). The over-approximation of $R^\theta(t; x_0)$ attained from applying Theorem 1 with decomposition functions for (29) and (30) is shown in blue. The over-approximation of $R^\theta(t; x_0)$ attained from applying Theorem 1 with the transformed first subsystem (36) is shown in red. Note that applying a linear transformation to the subsystem dynamics allows for higher fidelity reachable set computations. The initial state $x_0 = (q_0, \omega_0)$ given by (35) is shown in blue, and the deterministic trajectory $\theta(\Phi^F(t; x_0, 0))$, arising from the case with no disturbances, is shown in black.

- [8] S. Coogan and M. Arcak, “Efficient finite abstraction of mixed monotone systems,” in *Proceedings of the 18th International Conference on Hybrid Systems: Computation and Control*, pp. 58–67, 2015.
- [9] H. Smith, *Monotone Dynamical Systems: An Introduction to the Theory of Competitive and Cooperative Systems*. Mathematical surveys and monographs, American Mathematical Society, 2008.
- [10] D. Angeli and E. D. Sontag, “Monotone control systems,” *IEEE Transactions on Automatic Control*, vol. 48, pp. 1684–1698, Oct 2003.
- [11] M. Dutreix and S. Coogan, “Specification-guided verification and abstraction refinement of mixed monotone stochastic systems,” *IEEE Transactions on Automatic Control*, vol. 66, no. 7, pp. 2975–2990, 2021.
- [12] M. D. H. Dutreix, *Verification and synthesis for stochastic systems with temporal logic specifications*. PhD thesis, Georgia Institute of Technology, 2020.
- [13] M. Abate and S. Coogan, “Enforcing safety at runtime for systems with disturbances,” in *2020 59th IEEE Conference on Decision and Control (CDC)*, pp. 2038–2043, IEEE, 2020.
- [14] C. Llanes, M. Abate, and S. Coogan, “Safety from in-the-loop reachability for cyber-physical systems,” in *2021 Workshop on Computation-Aware Algorithmic Design for Cyber-Physical Systems (CAADCPS)*, CPS-IoT week, 2021.
- [15] M. Abate and S. Coogan, “Computing robustly forward invariant sets for mixed-monotone systems,” in *2020 59th IEEE Conference on Decision and Control (CDC)*, pp. 4553–4559, 2020.
- [16] M. Abate, M. Dutreix, and S. Coogan, “Tight decomposition functions for continuous-time mixed-monotone systems with disturbances,” *IEEE Control Systems Letters*, vol. 5, no. 1, pp. 139–144, 2021.
- [17] K. Shen, D. L. Robertson, and J. K. Scott, “Tight reachability bounds for constrained nonlinear systems using mean value differential inequalities,” *Automatica*, vol. 134, p. 109911, 2021.
- [18] L. Jaulin, M. Kieffer, O. Didrit, and E. Walter, “Applied interval analysis,” Springer, 2001.
- [19] M. Arcak, C. Meissen, and A. Packard, *Networks of dissipative systems: compositional certification of stability, performance, and safety*. Springer, 2016.
- [20] S. Coogan, “Mixed monotonicity for reachability and safety in dynamical systems,” in *2020 59th IEEE Conference on Decision and Control (CDC)*, pp. 5074–5085, 2020.
- [21] M. Khajenejad and S. Z. Yong, “Tight remainder-form decomposition functions with applications to constrained reachability and interval observer design,” 2021.
- [22] M. Abate and S. Coogan, “Improving the fidelity of mixed-monotone reachable set approximations via state transformations,” in *2021 American Control Conference (ACC)*, pp. 4674–4679, 2021.